

# Brain Angiogenesis Induced by Nonviral Gene Therapy with Potential Therapeutic Benefits for Central Nervous System Diseases

Idoia Gallego,<sup>▽</sup> Iliá Villate-Beitia,<sup>▽</sup> Cristina Soto-Sánchez, Margarita Menéndez, Santiago Grijalvo, Ramón Eritja, Gema Martínez-Navarrete, Lawrence Humphreys, Tania López-Méndez, Gustavo Puras,\* Eduardo Fernández, and José Luis Pedraz\*

Cite This: *Mol. Pharmaceutics* 2020, 17, 1848–1858

Read Online

ACCESS |

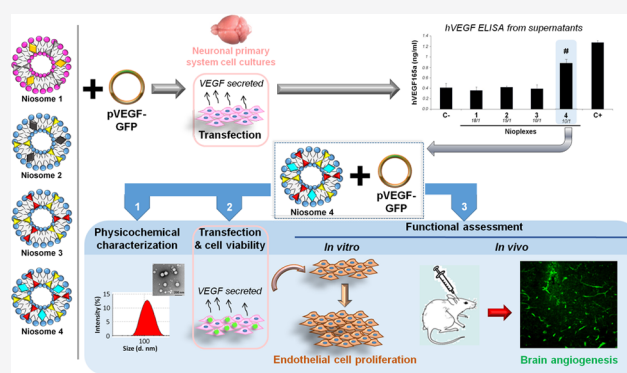
Metrics & More

Article Recommendations

Supporting Information

**ABSTRACT:** Gene therapy employing nanocarriers represents a promising strategy to treat central nervous system (CNS) diseases, where brain microvasculature is frequently compromised. Vascular endothelial growth factor (VEGF) is a key angiogenic molecule; however, its *in vivo* administration to the CNS by nonviral gene therapy has not been conducted. Hence, we prepared and physicochemically characterized four cationic niosome formulations (1–4), which were combined with pVEGF-GFP to explore their capacity to transfer the VEGF gene to CNS cells and achieve angiogenesis in the brain. Experiments in primary neuronal cells showed successful and safe transfection with niosome 4, producing double levels of biologically active VEGF in comparison to the rest of the formulations. Intracortical administration of niosome 4 based nioplexes in mouse brain validated the ability of this nonviral vector to deliver the VEGF gene to CNS cells, inducing brain angiogenesis and emerging as a promising therapeutic approach for the treatment of CNS diseases.

**KEYWORDS:** nonviral vector, niosomes, VEGF, gene therapy, angiogenesis, central nervous system



## 1. INTRODUCTION

Therapies based on gene therapy approaches have emerged as potential tools for the treatment of many congenital, acquired, and age-related diseases. Among the aforementioned ones, the prevalence of neurodegenerative disorders, in particular Alzheimer's disease (AD), is worryingly on the rise in first world countries along with the increase in life expectancy.<sup>1</sup> Nowadays there is no curative pharmacological treatment for these illnesses and the existing conventional ones can only slow down the progression of the disease. In this regard, recent advances in the field of nanotechnology and gene therapy represent a promising approach to face these diseases by the use of nanocarriers able to deliver therapeutic genetic material into target cells.<sup>2</sup>

The underlying cause of CNS maladies such as neurodegenerative diseases and stroke, among others, is still not fully understood as many factors are involved in the progression of their physiopathology. Nevertheless, it is becoming increasingly evident that the dysfunction and loss of cerebral microvasculature strongly contribute to the pathogenesis.<sup>3–5</sup> In this context, the vascular endothelial growth factor (VEGF) is a neuroprotective cytokine that regulates angiogenesis, blood–brain barrier (BBB) integrity, and neurogenesis in the CNS.<sup>6,7</sup> Therefore, VEGF represents a key molecule for

neuroprotection against neurological disorders by the therapeutic induction of vascular growth.<sup>8–10</sup> However, its healing use in a safe and controlled manner, along with the implementation of a proper gene therapy strategy, is a major hurdle to overcome in order to reach clinical use.<sup>11</sup> In this regard, nonviral vectors and in particular niosomes, represent a safe, low immunogenic, and low cytotoxic approach, easy to manufacture.<sup>12,13</sup> Basically, niosomes are composed of a cationic lipid, a “helper” component, and nonionic surfactants, which in combination confer to niosomes suitable characteristics for gene delivery, such as the capacity to bind DNA (forming the named nioplexes), proper physicochemical properties, and long-term stability.<sup>14–18</sup> Moreover, unlike viral vectors, no additional genes are inserted into target cells leading to a shift in preference to nonviral based products in preclinical trials.<sup>19–21</sup> In the last years, niosomes have achieved

Received: November 27, 2019

Revised: April 14, 2020

Accepted: April 15, 2020

Published: April 15, 2020



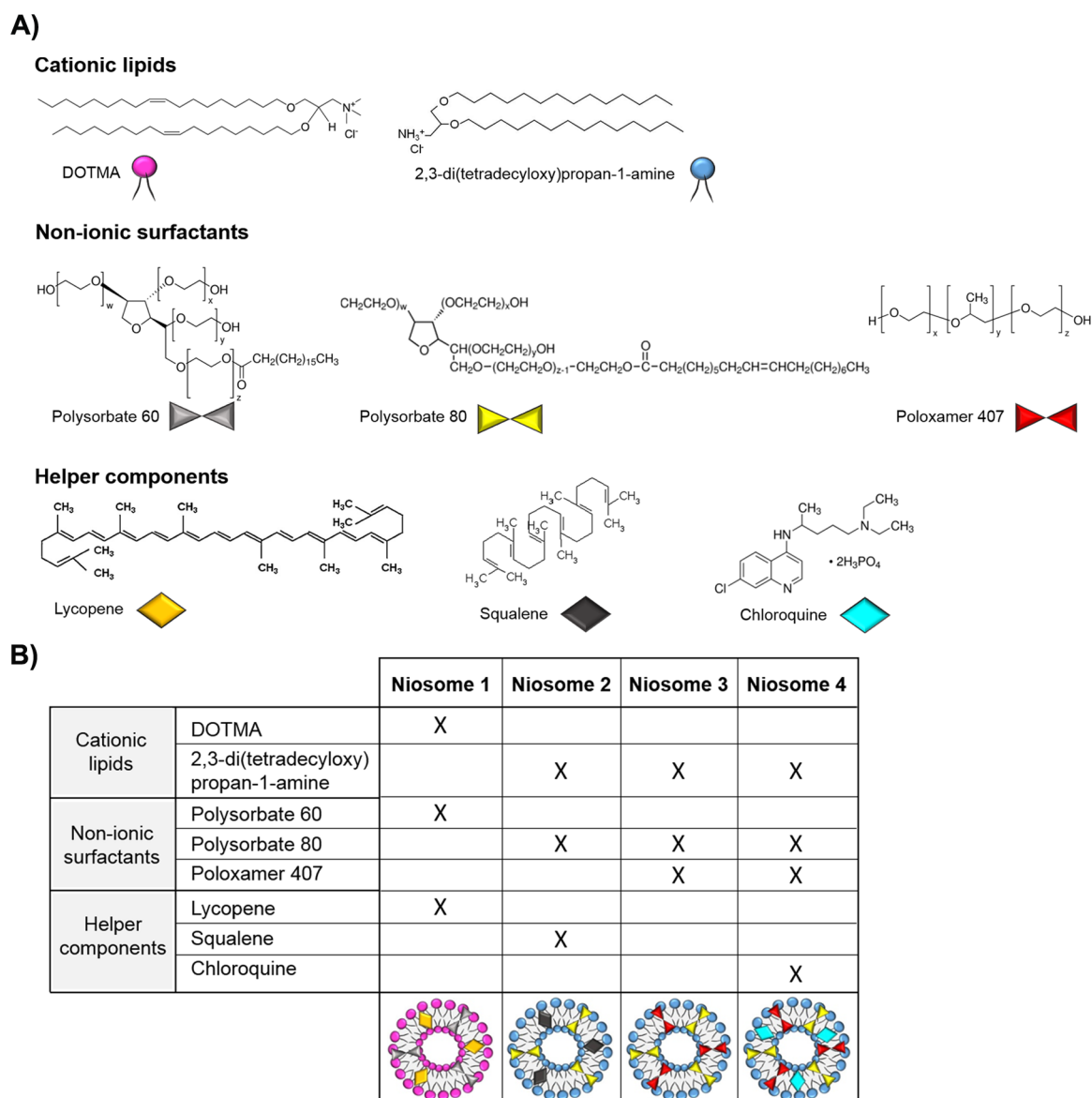


**Figure 1.** Scheme of the (A) chemical structures of the components and (B) composition of the niosome formulations.

encouraging results as gene delivery tools,<sup>18,22–25</sup> and focusing on the CNS, some works have demonstrated their capacity to transfer genetic material to CNS cells.<sup>26–28</sup> Regarding VEGF-encoding DNA transfection, even though some studies have employed nonviral strategies to achieve its delivery,<sup>29–31</sup> the *in vivo* gene therapy application of niosomes and VEGF in the CNS has not been explored.

Accordingly, the aim of the present work is to assess and select a niosome formulation able to efficiently transfer to the CNS the therapeutic VEGF genetic material to promote angiogenesis. For that purpose, we based our study on previously explored components for the development of niosome formulations<sup>23,24,32,33</sup> and analyzed their capacity to transfect a plasmid encoding VEGF (pVEGF-GFP) into primary neuronal cells extracted from rat embryo brains. The most efficient niosome was physicochemically characterized in terms of size, dispersity ( $\bar{D}$ ),  $\zeta$  potential, morphology, and molecular interactions with the genetic material. Transfection of pVEGF-GFP into primary neuronal cells employing this niosome was analyzed qualitatively and quantitatively, as well

as the cytotoxicity caused by the process. The biological activity of the VEGF protein secreted by transfected cells was evaluated by a proliferation assay in human umbilical vein cells (HUVEC), exposing them to the supernatant of transfected cells. Afterward, *in vivo* assays were performed in mouse brains injecting niosomes complexed to pVEGF-GFP at the intracortical level to analyze blood vessel genesis.

## 2. EXPERIMENTAL SECTION

### 2.1. Elaboration of Cationic Niosomes and Nioplexes.

All niosome formulations were elaborated by the oil-in-water emulsification technique following the same procedure described previously in the literature, with slight modifications. More specifically, in the case of niosome 1, 5 mg of cationic lipid DOTMA and 26 mg of polysorbate 60 (0.5%, w/v) mixed with 1 mg of lycopene were dissolved in 1 mL of dichloromethane as organic solvent and then emulsified with 5 mL of Milli-Q water.<sup>23</sup> For niosome 2, 5 mg of the 2,3-di(tetradecyloxy)propan-1-amine cationic lipid were dissolved in 1 mL of organic solvent dichloromethane (0.5%, w/v)

containing 20  $\mu\text{L}$  of squalene as “helper component” and then emulsified in 5 mL of an aqueous phase with polysorbate 80 as nonionic surfactant (0.5%, w/v).<sup>24</sup> In the case of niosome 3, 5 mg of the hydrochloride salt of the cationic lipid 2,3-di(tetradecyloxy)propan-1-amine with 12.5 mg of both poloxamer 407 and polysorbate 80 nonionic surfactants were dissolved in 1 mL of dichloromethane organic solvent and then sonicated in 5 mL of Milli-Q water.<sup>32</sup> Finally, niosome 4, was elaborated as niosome 3, but in this case, chloroquine (0.05%, w/v) was incorporated into the aqueous phase as a “helper” component.<sup>33</sup> A schematic representation of both the chemical structure of the components and the composition of each niosome formulation is shown in Figure 1. Briefly, emulsions were obtained by sonication (Branson Sonifier 250, Danbury) for 30 s at 50 W. Next, the dichloromethane organic solvent was removed from the emulsion by evaporation under magnetic agitation for 3 h at room temperature, obtaining the niosome colloidal suspensions.

Nioplexes were obtained incubating each niosome colloidal suspension with human VEGF-GFP plasmid (Sino Biological Inc., Beijing, China). The plasmid was expanded and purified using the Qiagen endotoxin-free plasmid purification Maxi-prep kit (Qiagen, California, USA) according to the manufacturer's instructions. The concentration of the purified plasmid was quantified in a SimpliNano spectrophotometer device (GE Healthcare, Buckinghamshire, UK). Then, an appropriate volume of pVEGF-GFP was mixed and incubated for 30 min at room temperature with the corresponding volume of each niosome suspension (1 mg/mL cationic lipid) to obtain the respective nioplexes at cationic lipid/DNA ratios (w/w) of 18/1 for niosome 1, 15/1 for niosome 2, 10/1 for niosome 3, and 10/1 for niosome 4.

**2.2. Physicochemical Characterization of Niosomes and Nioplexes.** Both the intensity mean diameter ( $Z$ -average) and the dispersity ( $\mathcal{D}$ ) were determined by dynamic light scattering, while the zeta potential was measured by laser Doppler velocimetry in a Zetasizer Nano ZS (Malvern Instruments, UK) after resuspension of the samples into NaCl 0.1 mM solution. The particle size, reported as hydrodynamic diameter, was achieved by cumulative analysis. The zeta potential was calculated from the electrophoretic mobility by the Smoluchowski approximation. All measurements were carried out in triplicate.

The shape and appearance of niosomes was assessed by transmission electron microscopy (TEM) as previously described.<sup>23</sup> The ability of niosomes to bind, release, and protect from enzymatic digestion the genetic material was analyzed by a gel retardation assay as previously described.<sup>18</sup> Naked DNA was used as control for each condition, the amount of DNA per well being 200 ng in all cases. Images were obtained with a ChemiDoc™ MP Imaging System and analyzed by Image Lab Software (BioRad, USA).

The interaction of niosomes and CQ with pVEGF-GFP was monitored by isothermal titration calorimetry (ITC) using a MicroCal PEAQ-ITC microcalorimeter (Malvern Instruments, UK). The assay was carried out at 25 °C by stepwise injection of niosomes (1 mg/mL cationic lipid) or chloroquine (CQ, 0.5 mg/mL) into the reaction cell loaded with an aqueous solution of pVEGF-GFP (0.0166 mg/mL). Typically, 1  $\times$  0.4  $\mu\text{L}$  injection followed by 3  $\times$  2  $\mu\text{L}$  and 11  $\times$  3  $\mu\text{L}$  injections were carried out automatically under 750 rpm stirring. The heat contributed by niosome or CQ dilution was measured in

separate runs and subtracted from the total heat produced following each injection prior to the data analysis.

**2.3. Animal Models.** E17–E18 rat embryos (Sprague–Dawley) were employed for the extraction of primary neuronal cells for *in vitro* experiments. ICR (CD-1, Envigo, Netherlands) mice were employed as the experimental animal model for *in vivo* assays. All experimental procedures were carried out in accordance with the RD 53/2013 Spanish and 2010/63/EU European Union regulations for the use of animals in scientific research. Procedures were approved and supervised by the Miguel Hernández University Standing Committee for Animal Use in the Laboratory, with code UMH.IB.EFJ.03.19/02.18.

**2.4. Primary Neuronal Cell Extraction and Culture.** Primary neuronal cells were extracted from the cortical tissue of E17–E18 rat embryos (Sprague–Dawley)<sup>29</sup> and maintained in DMEM (GIBCO, Thermofisher Scientific, MA, USA) with 10% fetal bovine serum (FBS, Biowest, Nuaille, France) during extraction. Afterward, chemical dissociation was carried out in FBS-free DMEM adding trypsin and incubating the mixture at 37 °C. Once the cell density was quantified in a hemocytometer, cells were resuspended in Neurobasal/FBS (GIBCO) medium supplemented with B27, GlutaMAX, and penicillin–streptomycin (GIBCO) and seeded at 3  $\times$  10<sup>5</sup> cells per well in 12 well plates on glass coverslips. Cell culture was then maintained in an incubator at 37 °C and 5% CO<sub>2</sub>.

**2.5. In Vitro Transfection in Primary Neuronal Cell Culture.** Cells were seeded in the medium and incubated to achieve 70% of confluence at the time of transfection (11–13 days *in vitro*). Nioplexes, composed of niosomes and 1.25  $\mu\text{g}$  of pVEGF-GFP per well at their respective cationic lipid/DNA ratio (w/w), were formed by electrostatic interactions during 30 min at room temperature in serum-free OptiMEM solution (GIBCO). Transfection was carried out by exposing cells to nioplexes for 4 h at 37 °C in the incubator, followed by removal of the transfection medium and replacement with fresh medium. Lipofectamine 2000 (Invitrogen, California, USA) at 2/1 ratio was employed as positive control, while baseline cells incubated with OptiMEM for 4 h were used as negative control. Each condition was performed in triplicate.

VEGF-GFP expression was analyzed 48 h after the exposure of cells to nioplexes in order to qualitatively evaluate the transfection efficiency by immunocytochemistry.<sup>29</sup> Hoechst 33342 (Thermofisher Scientific) was employed to label the cell nuclei. Coverslips were mounted and fluorescence images were taken with laser-confocal microscopy (Leica TCS SPE Microsystems GmbH, Germany).

**2.6. VEGF Production Evaluation.** The quantity of VEGF (ng/mL) released by primary neuronal transfected cells to the supernatant was analyzed 48 h post-transfection using a Human VEGF<sub>165</sub> Standard ABTS ELISA Development kit (PeproTech EC Ltd., London, UK)<sup>29,34</sup> according to the manufacturer's instructions. The absorbance was read at 450 nm, with the reference wavelength set at 650 nm, in an Infinite M200 microplate reader (TECAN Trading AG, Männedorf, Switzerland) using the Tecan i-Control 1.7 software. All measurements were carried out in triplicate.

**2.7. VEGF Bioactivity Assay.** The bioactivity of VEGF protein was evaluated by exposing human umbilical vein endothelial cells (HUVEC), considered as the *in vitro* cell model for angiogenesis, to an equal volume of the supernatant of transfected primary neuronal cells containing the secreted VEGF. For that purpose, HUVEC cells at early passages were seeded into 96-well poly(L-lysine)-coated culture plates at a

density of  $5 \times 10^3$  cells/well with nonsupplemented Endothelial Cell Growth Basal Medium (EBM-2, Lonza) and incubated for 24 h in a 5% CO<sub>2</sub> incubator. Once the culture medium was removed, the cells were incubated with 100  $\mu$ L of fresh EBM-2 medium and 200  $\mu$ L of the aforementioned supernatant per well for 72 h in the incubator. Afterward, cell proliferation was determined using the Cell Counting Kit-8 (Sigma-Aldrich, Spain) following the manufacturer's recommendations. The absorbance was read as described above. All measurements were carried out in triplicate. The supernatant of primary neuronal cells transfected with Lipofectamine 2000 (Invitrogen, California, USA) was employed as positive control. The supernatant of nontransfected primary neuronal cells was used as a negative control. Each condition was performed in triplicate. Data were normalized related to the negative control.

**2.8. Cell Viability.** The cell viability of primary neuronal cell cultures after their exposure to nioplexes was analyzed 48 h post-transfection by the tetrazolium salt 3-[4,5-dimethylthiazol-2-yl]-2,5-diphenyl tetrazolium bromide (MTT; Sigma-Aldrich, Spain) colorimetric assay, and the absorbance was read in a Bio-Rad iMarkMicroplate Reader according to the manufacturer's instructions. All measurements were carried out in triplicate.

**2.9. In Vivo Administration of Nioplexes at Intracortical Level.** During the surgery, the animals' bodies were kept warm with a water thermal pad. Mice were pretreated with dexamethasone (1 mg/kg ip) 24 h prior to surgery. A new dosage was administrated 20 min prior to and 24 h after surgery. We drilled a small craniotomy to expose the dura mater and arachnoids and performed a minimally invasive incision to introduce a Hamilton 33-gauge needle.

A volume of 0.8  $\mu$ L of nioplexes, containing 100 ng of pVEGF-GFP (10/1 ratio), was injected into the brain of ICR (CD-1) mice ( $n = 3$ ) at the cortex level with a microsyringe 33-gauge needle (Hamilton Co., Reno, NV). Niosomes alone, with no plasmid, were injected at the same level of mouse brain as a control ( $n = 3$ ). After the injection, the needle remained in situ for 5 min before being withdrawn slowly. The contralateral brain hemisphere of mice with no injection was also employed as a negative control. The anesthesia was induced with ketamine (80 mg/kg, ip) and sedation with diazepam (5 mg/kg, ip) maintaining the anesthesia with a mix of oxygen and 2% of isoflurane during the surgery. The depth of the anesthesia was evaluated continuously by monitoring heart rate and blinking and toe pinch reflexes. Mice were pretreated with dexamethasone (1 mg/kg ip) 24 h prior to surgery. A new dosage was administrated 20 min prior surgery. Antibiotic (enrofloxacin 25 mg/kg, sc), anti-inflammatory, and analgesic drugs (meloxicam 2 mg/kg, buprenorphine 0.1 mg/kg sc) were administrated to animals postsurgery. Once the procedure was finished, the animals were housed in their own cages for 7 days in a temperature- and light-controlled animal room with a 12 h light/darkness cycle. All the animals survived and behaved normally, and no loss of weight was detected after the surgery or during the treatment.

**2.10. Evaluation of Angiogenesis in Mouse Brain.** One week after the injection of nioplexes at the cerebral cortex, animals were sacrificed and brain samples were processed<sup>35</sup> to evaluate the expression of endoglin/CD105 qualitatively and quantitatively by immunohistochemistry.

Brain slices were blocked with a mixture containing 10% normal bovine serum (Sigma-Aldrich, Spain) and 0.5% Triton

X-100 and then incubated overnight at 4 °C with rat anti-mouse endoglin/CD105 monoclonal antibody (MA5-23894, Thermofisher) at 16  $\mu$ L/mL. After washing with PBS, they were incubated with a secondary antibody, AlexaFluor 488 rabbit anti-rat (1:100 dilution, Invitrogen, Themofisher), and the cell nuclei were counterstained with Hoechst 33342 (Sigma-Aldrich, Spain). Immunohistochemistry images were acquired with a Leica TCS SPE laser-confocal microscope (Leica, Microsystems GmbH, Wetzlar, Germany).

Vessel density was quantified on two brain sections from each animal located close to the intracortical injection of niosome 4 nioplexes and controls. Five regions of interest were analyzed from each section. Vessels were identified using anti-endoglin/CD105 immunostaining, and the vascular density (ratio of vasculature area to total area) was quantified using Fiji, an open source image processing application,<sup>36</sup> and the Vessel Analysis plugin, which allows automatic calculation of the vascular density.

**2.11. Statistical Analysis.** Differences between two groups were evaluated using a Student's *t* test or a Mann–Whitney *U* test, as appropriate after evaluating normality with a Shapiro–Wilks test. For multiple comparison, a 1-way ANOVA followed by an HSD Tukey test was performed in normality conditions or a Kruskal–Wallis test followed by a Mann–Whitney *U* test in nonparametric conditions. Data are expressed as mean  $\pm$  SD. A *P* value <0.05 was considered statistically significant. Analyses were performed with the SPSS 15.0 statistical package.

### 3. RESULTS

#### 3.1. Physicochemical Characterization of Niosomes.

The physicochemical characteristics of niosomes 1–4 are summarized in Figure 2. Niosomes presented mean diameter sizes ranging from 45.6 nm (niosome 3) to 129.7 nm (niosome

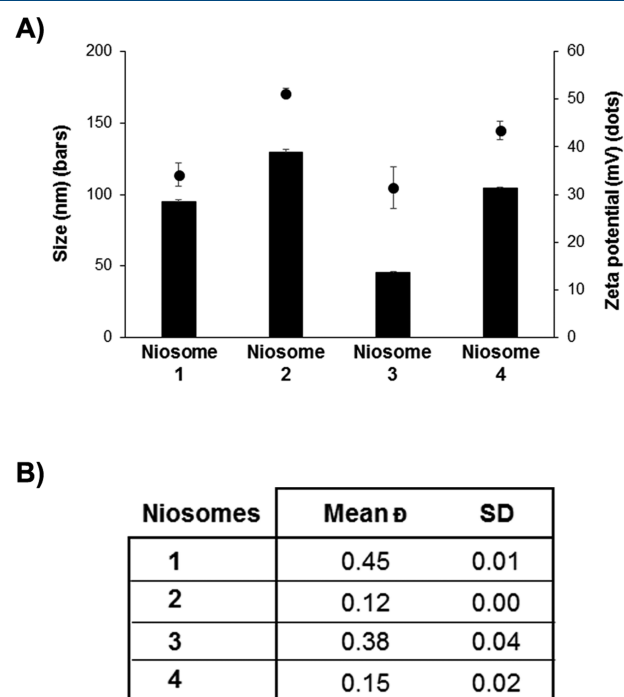


**Figure 2.** Physicochemical characterization of niosomes 1–4. (A) Size and zeta potential values. (B) Mean dispersity values. Each value represents the mean  $\pm$  SD from three measurements. Ø, dispersity.

2) and  $\zeta$  potentials over +30 mV. All  $\bar{D}$  were below 0.5 the most monodisperse formulations being those of niosomes 2 and 4 with values less than 0.2.

### 3.2. VEGF Release in Primary Neuronal Culture Cells.

The transfection of primary neuronal cells with nioplexes composed of niosomes 1–4 and pVEGF-GFP achieved VEGF release to supernatants. The analysis of VEGF concentration in these supernatants demonstrated that niosome 4 was the best formulation to efficiently transfect the genetic material into primary neuronal cells ( $P < 0.05$ ), releasing 0.9 ng/mL of VEGF within 48 h of the transfection (Figure 3) and doubling that of the rest of formulations.

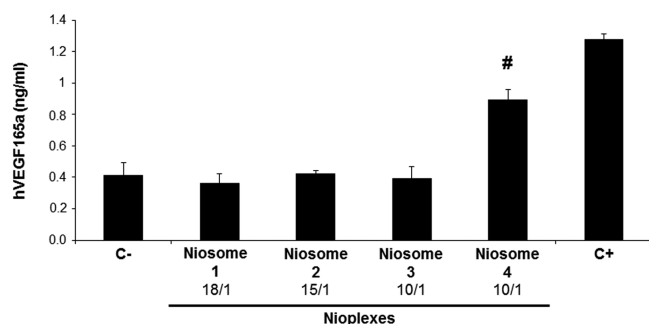


**Figure 3.** VEGF production (ng/mL) values by neuronal primary cell cultures 48 h post-transfection with nioplexes based on different niosomes (1–4) at fixed cationic lipid/pVEGF-GFP (w/w) ratios. Negative control cells (C–) were not treated with nioplexes. Positive control cells (C+) were transfected with Lipofectamine 2000. Each value represents the mean  $\pm$  SD,  $n = 3$ . #,  $P < 0.05$  compared with all conditions.

In fact, regarding niosome 4, it was later confirmed that 10/1 was the most effective cationic lipid/DNA ratio (w/w) for gene delivery in primary neuronal cells since VEGF levels found in their supernatants were 5-fold higher ( $P < 0.001$ ) than those obtained at lower ratios (2/1, 5/1) and there were no significant differences with those observed at higher ratios (15/1, 20/1, 30/1) (Supplementary Figure S1).

### 3.3. Characterization of Plasmid Binding to Niosome 4 Formulation.

Focusing on niosome 4 (Figure 4), when bound to pVEGF-GFP at 10/1 cationic lipid/DNA ratio (w/w), the mean diameter size increased by 77%, the  $\bar{D}$  increased slightly from 0.15 to 0.23, and zeta potential values decreased from +43.5 to +25.3 mV (Figure 4A). TEM capture (Figure 4B) showed a clear spherical morphology of these niosomes with no aggregates among them. The gel retardation assay (Figure 4C) showed that DNA complexed to niosome 4 at cationic lipid/DNA mass ratios 5/1, 10/1, and 15/1 was retained in the wells (lanes 3, 5, 7), while naked DNA completely migrated (lane 1). After the addition of DNase I and SDS to nioplexes (lanes 4, 6, 8), DNA migrated and intensive OC and SC bands were observed, contrary to lane 1, where the absence of visible bands indicated that naked DNA was totally degraded. The ITC profiles of complex formation between niosome 4 and pVEGF-GFP showed first an endothermic process, which dominates the thermal response at very low cationic lipid/pVEGF-GFP (w/w) ratios, and an exothermic component visible at ratios of 3 and above. This second process likely reflects the interaction of pVEGF-GFP with CQ, as inferred from the dose-dependent exothermic signal obtained upon direct titration of CQ into pVEGF-GFP (Figure 4C).

### 3.4. Gene Delivery, Cell Viability, and VEGF Bio-activity.

The qualitative analysis of transfection assays showed GFP signal in primary neuronal cells exposed to niosome 4 based nioplexes (Figure 5A) pointing to VEGF-GFP delivery into cells. The percentage of cell viability of primary neuronal cells upon transfection with these nioplexes was close to 100% of baseline and showed a higher rate ( $P < 0.01$ ) of living cells than Lipofectamine 2000 transfected cells (Figure 5B). HUVEC cells proliferated after their exposure to the VEGF present in the supernatant of transfected primary neuronal cells (Figure 5C). In particular, cell proliferation generated by VEGF was 25-fold more ( $P < 0.001$ ) compared with HUVEC negative control cells, and no significant differences in cell proliferation were found upon the exposure of HUVEC cells to the supernatant from cells transfected with niosome 4 based nioplexes and from Lipofectamine 2000 transfected cells (positive control).

### 3.5. Analysis of Angiogenesis *In Vivo*.

Endoglin/CD105 expression was found in mouse brain 1 week after intracortical injection of niosome 4 nioplexes vectoring pVEGF-GFP (Figure 6A, left), while only a slight signal was observed in niosome 4 alone injected control brains (Figure 6A, right). Interestingly, photomontages of immunohistochemistry sections showed that endoglin/CD105 signal was expressed in an extensive area in the vicinity of the injection point (Supplementary Figure S2). Quantitative data confirmed an increase of 76% ( $P < 0.001$ ) in vascular density in the brain of mice treated with niosome 4 and pVEGF-GFP ( $15.64 \pm 2.47$ ) compared with that of control ones ( $8.89 \pm 1.14$ ).

## 4. DISCUSSION

The high prevalence of neurodegenerative diseases, in which brain microvasculature is normally compromised, and the lack of conventional curative pharmacological treatments constitute an increasing worry worldwide. Approaches under research for the therapeutic treatment of neurological disorders include drug delivery employing poly(lactic-co-glycolic) acid nanoparticles that release the VEGF cytokine<sup>37</sup> or cell delivery by encapsulated VEGF-secreting cells.<sup>38</sup> However, they offer quick liberation kinetics with transient effects that might be interesting in acute pathological processes but not in the chronic ones. Since neurological maladies often involve a chronic status, a therapeutic treatment with sustained effects and preferably administered in a single dose is desirable. These features are provided by gene therapy strategies and, in fact, some of them consisting of viral vectors are currently commercialized for the treatment of other pathologies, such as Luxturna for Leber's congenital amaurosis.<sup>39</sup> Nevertheless, preclinical and clinical trials with viral vectors have evidenced severe symptoms associated with the high and uncontrolled expression of exogenous VEGF.<sup>40</sup> Therefore, nonviral approaches vectoring the gene of interest into the CNS represent a promising solution to all these hurdles. In the absence of research works about the *in vivo* implementation of nonviral gene therapy with VEGF in CNS, in this study cationic lipid based niosomes were employed to deliver VEGF-encoding DNA into CNS and, thus, promote angiogenesis as a therapeutic remedy for neurodegenerative disorders.

The formulations evaluated to this end, here named niosome 1, 2, 3, and 4, were elaborated by the oil-in-water emulsification technique, and the chemical composition of each niosome, along with the cationic lipid/DNA ratios (w/w), were based on optimization processes studied to deliver

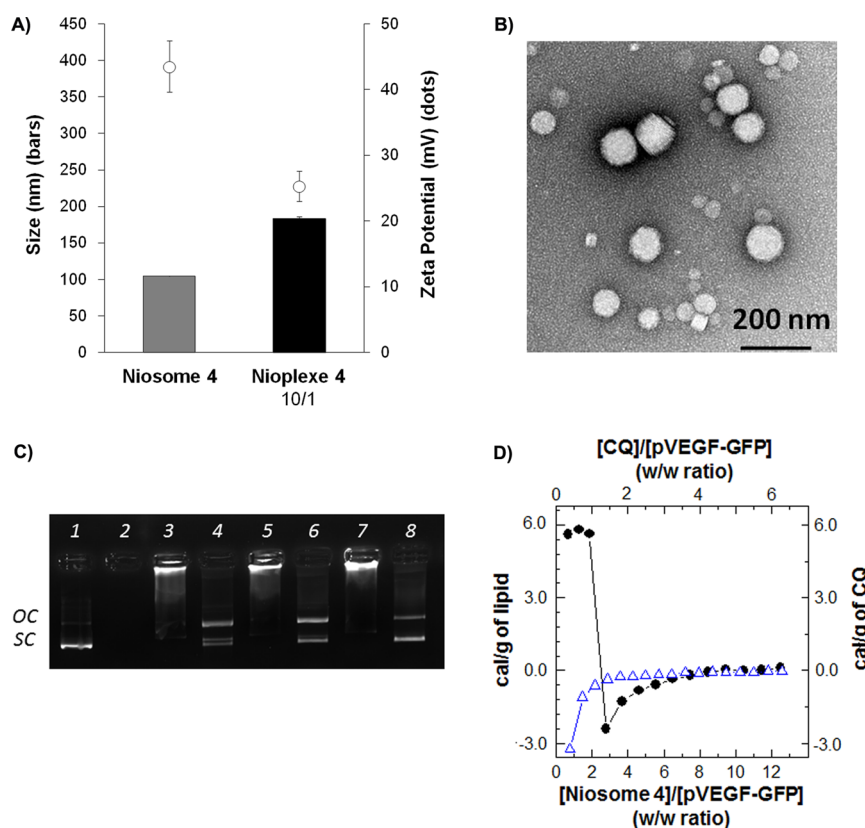


**Figure 4.** Physicochemical characterization of niosome 4 and of the corresponding nioplexes at 10/1 cationic lipid/pVEGF-GFP (w/w) ratio. (A) Size and zeta potential values. Each value represents the mean  $\pm$  SD from three measurements. (B) TEM image of niosome 4. Scale bar 200 nm. (C) Binding, protection, and SDS-induced release of DNA from nioplexes visualized by agarose gel electrophoresis. Lanes 1 and 2, free DNA; lanes 3 and 4, nioplexes at cationic lipid/DNA mass ratio 5/1; lanes 5 and 6, nioplexes at cationic lipid/DNA mass ratio 10/1; lanes 7 and 8, nioplexes at cationic lipid/DNA mass ratio 15/1. Free DNA and nioplexes were treated with DNase I + SDS (lanes 2, 4, 6, and 8). OC, open circular form; SC, supercoiled form. (D) ITC profile of niosome 4 titration into pVEGF-GFP. Circles show the heat evolved per gram of cationic lipid injected (left-hand side scale) versus the ratio of cationic lipid/DNA concentrations (bottom scale) after correcting for the contribution of niosome dilution. Triangles show the dependence of the heat evolved by gram of chloroquine (CQ) injected into pVEGF-GFP at 0.0166 mg/mL (right-hand side scale) with CQ/DNA concentration ratio (upper scale), at the concentrations used in nioplex formation. Bottom and top scales were matched to align the heats derived from CQ injection to those of niosome 4 injections. Solid lines illustrate the tendency of the ITC profiles.

fluorescence and luminescence reporter plasmids.<sup>23,24,32,33</sup> The physicochemical characterization of these niosomes was consistent with the data of the aforementioned studies and confirmed their suitability for gene therapy purposes, with mean diameters smaller than 200 nm, positive  $\zeta$  potentials to promote electrostatic interactions with the negatively charged genetic material, and low  $\bar{D}$  pointing to monodisperse niosome populations (Figure 2). However, the VEGF content in the supernatant of transfected primary neuronal cells showed that, among the four explored formulations, only niosome 4 was able to efficiently deliver the genetic material to CNS cells (Figure 3). This fact is consistent with literature asserting that niosome composition has a direct influence in its ability for transfection, depending on the cell type and the specific cellular internalization pathways.<sup>16,18,28,41</sup> In this particular case, the CQ content present in niosome 4 seems to play a key role, since it is the only difference in the composition compared with niosome 3 (Figure 1B), which showed a low transfection rate. In this concern, CQ could be promoting VEGF plasmid delivery in two ways. On the one hand, CQ has the ability to intercalate in the DNA and, therefore, protects the genetic material.<sup>42,43</sup> In fact, ITC data (Figure 4D, triangles) upholds this hypothesis of CQ interaction with the DNA, as the injection of CQ into pVEGF-GFP samples (upper

scale) produced an exothermic reaction (right-hand side scale) that compared to the exothermic component displayed by niosome 4 titration. On the other hand, once the genetic material is delivered to target cells, CQ can promote endosomal and lysosomal escape of the gene by the protonation of CQ at the low pH of these vesicles, avoiding their acidification and enzymatic function.<sup>44</sup> Therefore, the CQ component of niosome 4 might be promoting gene transfection in agreement with data obtained from other works, both *in vitro* and *in vivo*.<sup>45</sup>

Once the suitability of niosome 4 for gene delivery purposes in CNS cells was corroborated, this niosome was complexed to pVEGF-GFP at the optimal cationic lipid/DNA mass ratio 10/1 (Supplementary Figure S1) for further physicochemical and biological analysis. As predictable, the mean diameter increased and the positive  $\zeta$ eta potential decreased after complexing to pVEGF-GFP (Figure 4A) because of the partial neutralization of the positive amines of the niosomes by the phosphate groups of the genetic material.  $\bar{D}$  data and TEM captures (Figure 4B) revealed a narrow distribution and spherical shape of niosomes with no aggregates. All these factors contribute to create an adequate microenvironment that favors the stability, homogeneity, and interactions with DNA for gene therapy applications.<sup>41</sup> Interaction assays between the genetic material

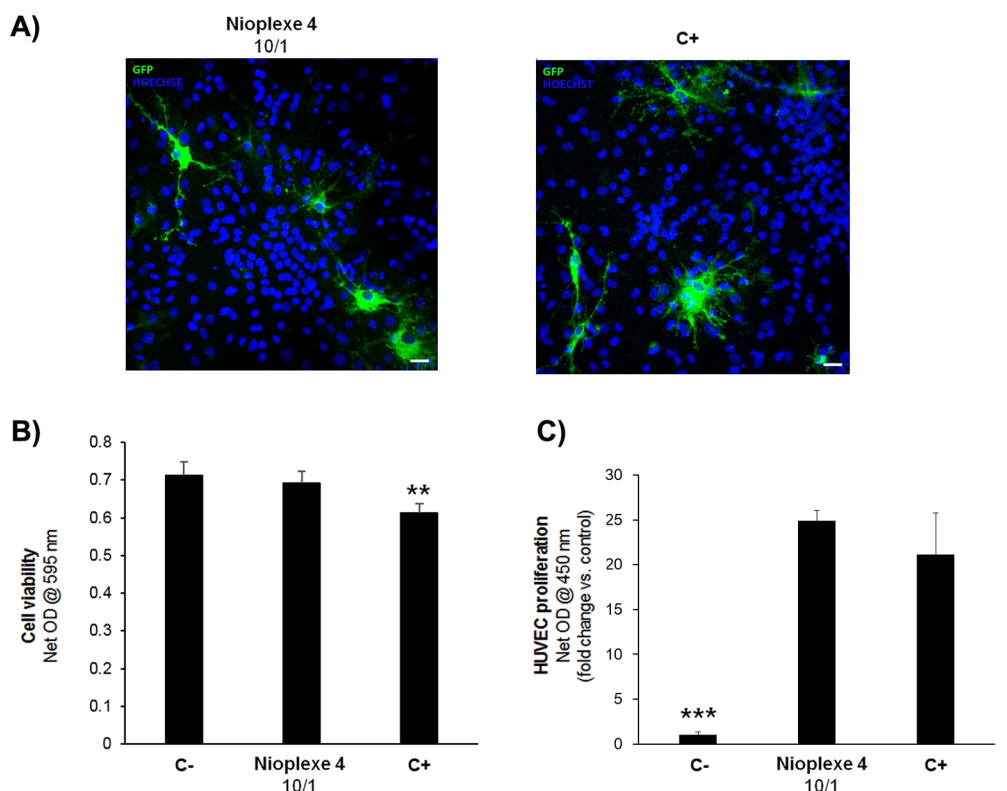


**Figure 5.** *In vitro* transfection experiments. (A) Fluorescence immunohistochemistry showing VEGF-GFP positive signal after transfection in primary neuronal culture cells with niosome 4 based nioplexes or Lipofectamine 2000 as positive control. Green, anti-GFP; blue, Hoechst. Scale bar: 20  $\mu\text{m}$ . (B) Cell viability assay of primary neuronal culture cells after transfection. Each value represents the mean  $\pm$  SD,  $n = 3$ .  $**P < 0.01$ , compared with the positive control. (C) Proliferation of HUVEC cells in response to the VEGF secreted by primary neuronal cells after transfection. Negative (C-) and positive (C+) controls represent HUVEC cells exposed to the supernatant of transfection control cells and of cells transfected with Lipofectamine 2000, respectively. Each value represents the mean  $\pm$  SD,  $n = 3$ .  $***P < 0.001$  compared with the negative control.

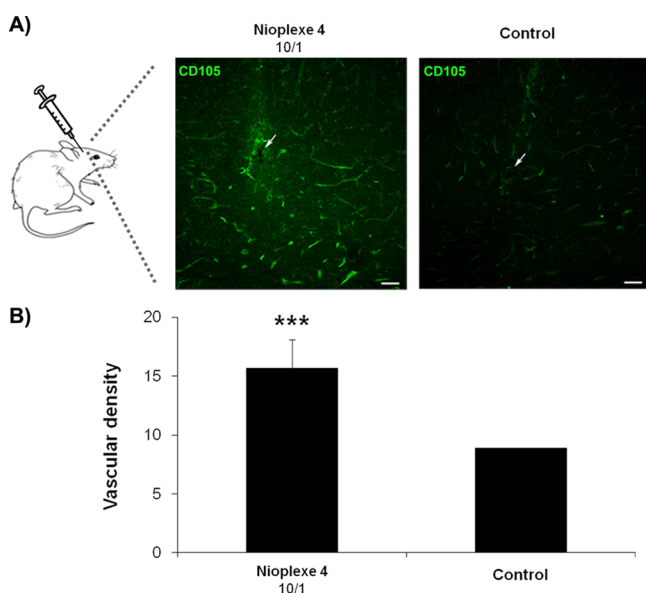


**Figure 6.** *In vivo* assays showing brain angiogenesis after injection of nioplexes inside the cerebral cortex of ICR (CD-1) mice. (A) Fluorescence immunohistochemistry in brain sections showing endoglin/CD105 positive signal after administration of nioplexes composed by niosome 4 and pVEGF-GFP or niosome 4 alone as control. Scale bar: 40  $\mu\text{m}$ . White arrows mark the injection point. (B) Quantification of the vascular density. Each value represents the mean  $\pm$  SD,  $***P < 0.001$ .

and niosome 4 showed that, on the one hand, this vector has the capacity to condense and protect pVEGF-GFP from enzymatic digestion, as well as maintain a suitable balance between DNA binding and releasing abilities at all cationic lipid/DNA mass ratios tested (Figure 4C). On the other hand, ITC assays also demonstrated that interactions between niosome 4 and pVEGF-GFP (Figure 4D, circles) reached saturation at 12/1 (w/w) ratio (bottom scale vs left-hand side scale), thereby explaining why transfection assays in primary neuronal cells exhibited maximal efficiency at niosome to DNA ratios of around 10/1 with no perceptible differences with higher ratios of 15/1, 20/1, and 30/1, as can be observed in Supplementary Figure S1. Since the use of higher ratios involves decreasing the amount of plasmid that can be administered by cortex injection into mouse brain, which is limited by the volume of the complexes, and because there was not significant increase in VEGF production at higher ratios, 10/1 cationic lipid/DNA ratio was selected for further experiments.

Additional biological studies were performed with niosome 4 at 10/1 cationic lipid/DNA ratio (w/w) in order to analyze the gene delivery capacity of the transfection process, the possible harmfulness of nioplex exposure to cells, and the bioactivity of the VEGF secreted by primary neuronal cells after transfection. VEGF-GFP expression in primary neuronal cell cultures revealed the ability of nioplexes to successfully deliver the genetic material to this cell type (Figure 5A). The commercial liposome Lipofectamine 2000 was employed as a positive control of transfection; however, cell viability data

clearly showed the toxic feature of this vector since the rate of cell viability was reduced by 15% after transfection as compared with the one of niosome 4, which maintained cell viability very close to that of negative control cells (Figure 5B). This lower toxicity of niosomes is one of their main advantages over liposomes, as the latter possess phospholipids that confer a too high positive charge on their surface, contributing to cell death, both *in vitro* and *in vivo*.<sup>46,47</sup> Importantly, the VEGF produced by transfected cells preserved its biological activity (Figure 5C) as observed in the proliferation assay performed with the *in vitro* model for angiogenesis, HUVEC cells, which have previously been employed to evaluate the biological function of VEGF upon transfection of CNS cells.<sup>29</sup>

*In vivo* administration of nioplexes based on niosome 4 and pVEGF-GFP was performed in mouse brain by injection at the intracortical level. The immunohistological analysis of brain sections showed positive expression of CD105 (Figure 6A), pointing to new blood vessel formation not only at the injection point but also in a wide area in its vicinity (Supplementary Figure 2S). In fact, angiogenesis was confirmed by the quantification of the vascular density, showing almost doubling of vessels compared with that found in control mice (Figure 6B). The slight CD105 expression presented by the negative control mouse brain sections could be explained as the physiological response to the injury caused by the injection *per se*. In this respect, even though injection is not the first choice for a therapeutic treatment due to its invasiveness, other approaches such as intranasal administration could represent a promising alternative to current nonviral based strategies for brain targeting, as demonstrated in studies where these vectors were administered by the intranasal route in rats.<sup>48,49</sup> It is noteworthy that the administration of nioplexes was conducted in mouse brain without pathology. Hence, it is quite likely that the angiogenesis promoted by VEGF gene delivery is balanced by other antiangiogenic factors to maintain the vasculature in a quiescent state. In this regard, nonviral VEGF gene therapy would be particularly interesting for the treatment of AD, since multiple lines of evidence indicate an important vascular contribution in the development of this pathology.<sup>50</sup> In fact, several genetic and neuropathological studies have shown that genes identified as cardiovascular risk factors are also related to AD risk<sup>51</sup> and that around 80% of AD patients present vascular pathologies such as microinfarcts and atherosclerosis of cerebral arteries,<sup>52,53</sup> respectively. Additionally, morphological changes at the microvascular level have also been observed in AD animal models.<sup>54</sup> Therefore, considering the specific roles that VEGF plays in brain angiogenesis, BBB integrity, and neuroprotection, its upregulation via gene therapy seems a promising strategy for the treatment of AD.

## 5. CONCLUSIONS

The nonviral vector niosome 4 presents physicochemical features suitable for gene therapy purposes in the CNS. In addition, niosome 4 efficiently transfects VEGF with biological activity to CNS cells in a safe manner, not only in primary neuronal cell cultures but also in mouse brain, promoting angiogenesis after injection. Hence, niosome 4 in combination with VEGF-encoding DNA is a potential tool for restoring brain microvasculature, which could ultimately promote BBB integrity and neuroprotection against neurological disorders. Hence, this study represents a proof of concept to promote

new blood vessel formation in mouse brain by nonviral gene therapy, which could have further clinical applications.

## ■ ASSOCIATED CONTENT

### Supporting Information

The Supporting Information is available free of charge at <https://pubs.acs.org/doi/10.1021/acs.molpharmaceut.9b01213>.

VEGF production after transfection with nioplexes based on niosome 4 at different cationic lipid/pVEGF-GFP (w/w) ratios and immunohistochemistry sections against endoglin/CD105 after injecting nioplexes based on niosome 4 or niosome 4 alone inside the cerebral cortex of mouse brain (PDF)

## ■ AUTHOR INFORMATION

### Corresponding Authors

**Gustavo Puras** – NanoBioCel Group, University of the Basque Country (UPV/EHU), Vitoria-Gasteiz 01006, Spain; Biomedical Research Networking Center in Bioengineering, Biomaterials and Nanomedicine (CIBER-BBN), Madrid 28029, Spain; [orcid.org/0000-0002-1536-7601](https://orcid.org/0000-0002-1536-7601); Phone: + (34)-945014536; Email: [gustavo.puras@ehu.eus](mailto:gustavo.puras@ehu.eus)

**José Luis Pedraz** – NanoBioCel Group, University of the Basque Country (UPV/EHU), Vitoria-Gasteiz 01006, Spain; Biomedical Research Networking Center in Bioengineering, Biomaterials and Nanomedicine (CIBER-BBN), Madrid 28029, Spain; Phone: + (34)-945013091; Email: [joseluis.pedraz@ehu.eus](mailto:joseluis.pedraz@ehu.eus); Fax: +34 945013040

### Authors

**Idoia Gallego** – NanoBioCel Group, University of the Basque Country (UPV/EHU), Vitoria-Gasteiz 01006, Spain; Biomedical Research Networking Center in Bioengineering, Biomaterials and Nanomedicine (CIBER-BBN), Madrid 28029, Spain

**Ilia Villate-Beitia** – NanoBioCel Group, University of the Basque Country (UPV/EHU), Vitoria-Gasteiz 01006, Spain; Biomedical Research Networking Center in Bioengineering, Biomaterials and Nanomedicine (CIBER-BBN), Madrid 28029, Spain

**Cristina Soto-Sánchez** – Biomedical Research Networking Center in Bioengineering, Biomaterials and Nanomedicine (CIBER-BBN), Madrid 28029, Spain; Neuroprosthesis and Neuroengineering Research Group, Miguel Hernández University, Elche 03202, Spain

**Margarita Menéndez** – Rocasolano Physical Chemistry Institute, Superior Council of Scientific Investigations (IQFR-CSIC), Madrid 28006, Spain; Biomedical Research Networking Center in Respiratory Diseases (CIBERES), Madrid 28029, Spain

**Santiago Grijalvo** – Biomedical Research Networking Center in Bioengineering, Biomaterials and Nanomedicine (CIBER-BBN), Madrid 28029, Spain; Institute of Advanced Chemistry of Catalonia (IQAC-CSIC), Barcelona 08034, Spain

**Ramón Eritja** – Biomedical Research Networking Center in Bioengineering, Biomaterials and Nanomedicine (CIBER-BBN), Madrid 28029, Spain; Institute of Advanced Chemistry of Catalonia (IQAC-CSIC), Barcelona 08034, Spain;

[orcid.org/0000-0001-5383-9334](https://orcid.org/0000-0001-5383-9334)

**Gema Martínez-Navarrete** – Biomedical Research Networking Center in Bioengineering, Biomaterials and Nanomedicine

(CIBER-BBN), Madrid 28029, Spain; Neuroprosthesis and Neuroengineering Research Group, Miguel Hernández University, Elche 03202, Spain

**Lawrence Humphreys** – Biomedical Research Networking Center in Bioengineering, Biomaterials and Nanomedicine (CIBER-BBN), Madrid 28029, Spain; Neuroprosthesis and Neuroengineering Research Group, Miguel Hernández University, Elche 03202, Spain

**Tania López-Méndez** – NanoBioCel Group, University of the Basque Country (UPV/EHU), Vitoria-Gasteiz 01006, Spain; Biomedical Research Networking Center in Bioengineering, Biomaterials and Nanomedicine (CIBER-BBN), Madrid 28029, Spain

**Eduardo Fernández** – Biomedical Research Networking Center in Bioengineering, Biomaterials and Nanomedicine (CIBER-BBN), Madrid 28029, Spain; Neuroprosthesis and Neuroengineering Research Group, Miguel Hernández University, Elche 03202, Spain

Complete contact information is available at:

<https://pubs.acs.org/10.1021/acs.molpharmaceut.9b01213>

### Author Contributions

<sup>†</sup>I.G. and I.V.-B. contributed equally to this work.

### Funding

This work was supported by the Basque Country Government (Department of Education, University and Research, predoctoral grant PRE\_2016\_2\_0302 and Consolidated Groups, IT907-16), the Spanish Grant RTI2018-098969-B-100 and the Research Chair “Bidons Egara”. Additional funding was provided by the CIBER of Bioengineering, Biomaterials and Nanomedicine (CIBER-BBN) and Respiratory Diseases (CIBERES), an initiative of the Carlos III Health Institute (ISCIII).

### Notes

The authors declare no competing financial interest.

## ■ ACKNOWLEDGMENTS

Authors thank the intellectual and technical assistance from the ICTS “NANBIOSIS”, more specifically by the Drug Formulation Unit (U10) of the CIBER in Bioengineering, Biomaterials and Nanomedicine (CIBER-BBN) at the University of the Basque Country (UPV/EHU). Technical and human support provided by SGIker (UPV/EHU) and European funding (ERDF and ESF) is gratefully acknowledged, as is Dr. José Manuel Andreu (CIB-CSIC) for supplying access to PEAQ-ITC equipment.

## ■ ABBREVIATIONS

CNS, central nervous system; p, plasmid; VEGF, vascular endothelial growth factor; GFP, green fluorescent protein; Đ, dispersity; TEM, transmission electron microscopy; ITC, isothermal titration calorimetry; CQ, chloroquine; FBS, fetal bovine serum

## ■ REFERENCES

- (1) Harper, S. Economic and social implications of aging societies. *Science* **2014**, *346*, 587–591.
- (2) Teleanu, D. M.; Negut, I.; Grumezescu, V.; Grumezescu, A. M.; Teleanu, R. I. Nanomaterials for Drug Delivery to the Central Nervous System. *Nanomaterials* **2019**, *9*, 371–389.
- (3) Sweeney, M. D.; Montagne, A.; Sagare, A. P.; Nation, D. A.; Schneider, L. S.; Chui, H. C.; Harrington, M. G.; Pa, J.; Law, M.;

Wang, D. J. J.; Jacobs, R. E.; Doubal, F. N.; Ramirez, J.; Black, S. E.; Nedergaard, M.; Benveniste, H.; Dichgans, M.; Iadecola, C.; Love, S.; Bath, P. M.; Markus, H. S.; Salman, R. A.; Allan, S. M.; Quinn, T. J.; Kalaria, R. N.; Werring, D. J.; Carare, R. O.; Touyz, R. M.; Williams, S. C. R.; Moskowitz, M. A.; Katusic, Z. S.; Lutz, S. E.; Lazarov, O.; Minshall, R. D.; Rehman, J.; Davis, T. P.; Wellington, C. L.; Gonzalez, H. M.; Yuan, C.; Lockhart, S. N.; Hughes, T. M.; Chen, C. L. H.; Sachdev, P.; O'Brien, J. T.; Skoog, I.; Pantoni, L.; Gustafson, D. R.; Biessels, G. J.; Wallin, A.; Smith, E. E.; Mok, V.; Wong, A.; Passmore, P.; Barkof, F.; Muller, M.; Breteler, M. M. B.; Roman, G. C.; Hamel, E.; Seshadri, S.; Gottesman, R. F.; van Buchem, M. A.; Arvanitakis, Z.; Schneider, J. A.; Drewes, L. R.; Hachinski, V.; Finch, C. E.; Toga, A. W.; Wardlaw, J. M.; Zlokovic, B. V. Vascular dysfunction-The disregarded partner of Alzheimer's disease. *Alzheimer's Dementia* **2019**, *15*, 158–167.

(4) van der Holst, H. M.; van Uden, I. W.; Tuladhar, A. M.; de Laat, K. F.; van Norden, A. G.; Norris, D. G.; van Dijk, E. J.; Esselink, R. A.; Platel, B.; de Leeuw, F. E. Cerebral small vessel disease and incident parkinsonism: The RUN DMC study. *Neurology* **2015**, *85*, 1569–1577.

(5) O'Donnell, M. E.; Yuan, J. X. Pathophysiology of stroke: the many and varied contributions of brain microvasculature. *Am. J. Physiol. Cell. Physiol.* **2018**, *315*, C341–C342.

(6) Zhang, Z. G.; Zhang, L.; Jiang, Q.; Zhang, R.; Davies, K.; Powers, C.; Bruggen, N.; Chopp, M. VEGF enhances angiogenesis and promotes blood-brain barrier leakage in the ischemic brain. *J. Clin. Invest.* **2000**, *106*, 829–838.

(7) Greenberg, D. A.; Jin, K. From angiogenesis to neuropathology. *Nature* **2005**, *438*, 954–959.

(8) Lange, C.; Storkebaum, E.; de Almodovar, C. R.; Dewerchin, M.; Carmeliet, P. Vascular endothelial growth factor: a neurovascular target in neurological diseases. *Nat. Rev. Neurol.* **2016**, *12*, 439–454.

(9) Shim, J. W.; Madsen, J. R. VEGF Signaling in Neurological Disorders. *Int. J. Mol. Sci.* **2018**, *19*, 275–297.

(10) Religa, P.; Cao, R.; Religa, D.; Xue, Y.; Bogdanovic, N.; Westaway, D.; Marti, H. H.; Winblad, B.; Cao, Y. VEGF significantly restores impaired memory behavior in Alzheimer's mice by improvement of vascular survival. *Sci. Rep.* **2013**, *3*, 2053.

(11) Lewandowski, A. J.; Davis, E. F.; Lazdam, M.; Leeson, P. From gene to epigene-based therapies targeting the vascular endothelium. *Curr. Vasc. Pharmacol.* **2012**, *10*, 125–137.

(12) Rajera, R.; Nagpal, K.; Singh, S. K.; Mishra, D. N. Niosomes: a controlled and novel drug delivery system. *Biol. Pharm. Bull.* **2011**, *34*, 945–953.

(13) Choi, W. J.; Kim, J. K.; Choi, S. H.; Park, J. S.; Ahn, W. S.; Kim, C. K. Low toxicity of cationic lipid-based emulsion for gene transfer. *Biomaterials* **2004**, *25*, 5893–5903.

(14) Karmali, P. P.; Chaudhuri, A. Cationic liposomes as non-viral carriers of gene medicines: resolved issues, open questions, and future promises. *Med. Res. Rev.* **2007**, *27*, 696–722.

(15) Dabkowska, A. P.; Barlow, D. J.; Campbell, R. A.; Hughes, A. V.; Quinn, P. J.; Lawrence, M. J. Effect of helper lipids on the interaction of DNA with cationic lipid monolayers studied by specular neutron reflection. *Biomacromolecules* **2012**, *13*, 2391–2401.

(16) Ojeda, E.; Puras, G.; Agirre, M.; Zarate, J.; Grijalvo, S.; Eritja, R.; DiGiacomo, L.; Caracciolo, G.; Pedraz, J. L. The role of helper lipids in the intracellular disposition and transfection efficiency of niosome formulations for gene delivery to retinal pigment epithelial cells. *Int. J. Pharm.* **2016**, *503*, 115–126.

(17) Taymouri, S.; Varshosaz, J. Effect of different types of surfactants on the physical properties and stability of carvedilol nano-niosomes. *Adv. Biomed. Res.* **2016**, *5*, 48.

(18) Villate-Beitia, I.; Gallego, I.; Martinez-Navarrete, G.; Zarate, J.; Lopez-Mendez, T.; Soto-Sanchez, C.; Santos-Vizcaino, E.; Puras, G.; Fernandez, E.; Pedraz, J. L. Polysorbate 20 non-ionic surfactant enhances retinal gene delivery efficiency of cationic niosomes after intravitreal and subretinal administration. *Int. J. Pharm.* **2018**, *550*, 388–397.

- (19) Ramamoorth, M.; Narvekar, A. Non viral vectors in gene therapy- an overview. *J. Clin. Diagn. Res.* **2015**, *9*, GE01–6.
- (20) Foldvari, M.; Chen, D. W.; Nafissi, N.; Calderon, D.; Narsineni, L.; Rafiee, A. Non-viral gene therapy: Gains and challenges of non-invasive administration methods. *J. Controlled Release* **2016**, *240*, 165–190.
- (21) Yin, H.; Kanasty, R. L.; Eltoukhy, A. A.; Vegas, A. J.; Dorkin, J. R.; Anderson, D. G. Non-viral vectors for gene-based therapy. *Nat. Rev. Genet.* **2014**, *15*, 541–555.
- (22) Attia, N.; Mashal, M.; Grijalvo, S.; Eritja, R.; Zarate, J.; Puras, G.; Pedraz, J. L. Stem cell-based gene delivery mediated by cationic niosomes for bone regeneration. *Nanomedicine* **2018**, *14*, 521–531.
- (23) Mashal, M.; Attia, N.; Puras, G.; Martinez-Navarrete, G.; Fernandez, E.; Pedraz, J. L. Retinal gene delivery enhancement by lycopene incorporation into cationic niosomes based on DOTMA and polysorbate 60. *J. Controlled Release* **2017**, *254*, 55–64.
- (24) Puras, G.; Mashal, M.; Zarate, J.; Agirre, M.; Ojeda, E.; Grijalvo, S.; Eritja, R.; Diaz-Tahoces, A.; Martinez Navarrete, G.; Aviles-Trigueros, M.; Fernandez, E.; Pedraz, J. L. A novel cationic niosome formulation for gene delivery to the retina. *J. Controlled Release* **2014**, *174*, 27–36.
- (25) Gallego, I.; Villate-Beitia, I.; Martinez-Navarrete, G.; Menendez, M.; Lopez-Mendez, T.; Soto-Sanchez, C.; Zarate, J.; Puras, G.; Fernandez, E.; Pedraz, J. L. Non-viral vectors based on cationic niosomes and minicircle DNA technology enhance gene delivery efficiency for biomedical applications in retinal disorders. *Nanomedicine* **2019**, *17*, 308–318.
- (26) Attia, N.; Mashal, M.; Soto-Sanchez, C.; Martinez-Navarrete, G.; Fernandez, E.; Grijalvo, S.; Eritja, R.; Puras, G.; Pedraz, J. L. Gene transfer to rat cerebral cortex mediated by polysorbate 80 and poloxamer 188 nonionic surfactant vesicles. *Drug Des., Dev. Ther.* **2018**, *12*, 3937–3949.
- (27) Mashal, M.; Attia, N.; Soto-Sanchez, C.; Martinez-Navarrete, G.; Fernandez, E.; Puras, G.; Pedraz, J. L. Non-viral vectors based on cationic niosomes as efficient gene delivery vehicles to central nervous system cells into the brain. *Int. J. Pharm.* **2018**, *552*, 48–55.
- (28) Ojeda, E.; Puras, G.; Agirre, M.; Zarate, J.; Grijalvo, S.; Eritja, R.; Martinez-Navarrete, G.; Soto-Sanchez, C.; Diaz-Tahoces, A.; Aviles-Trigueros, M.; Fernandez, E.; Pedraz, J. L. The influence of the polar head-group of synthetic cationic lipids on the transfection efficiency mediated by niosomes in rat retina and brain. *Biomaterials* **2016**, *77*, 267–279.
- (29) Villate-Beitia, I.; Puras, G.; Soto-Sanchez, C.; Agirre, M.; Ojeda, E.; Zarate, J.; Fernandez, E.; Pedraz, J. L. Non-viral vectors based on magnetoplexes, lipoplexes and polyplexes for VEGF gene delivery into central nervous system cells. *Int. J. Pharm.* **2017**, *521*, 130–140.
- (30) Chae, H. Y.; Lee, B. W.; Oh, S. H.; Ahn, Y. R.; Chung, J. H.; Min, Y. K.; Lee, M. S.; Lee, M. K.; Kim, K. W. Effective glycemic control achieved by transplanting non-viral cationic liposome-mediated VEGF-transfected islets in streptozotocin-induced diabetic mice. *Exp. Mol. Med.* **2005**, *37*, 513–523.
- (31) Curtin, C. M.; Tierney, E. G.; McSorley, K.; Cryan, S. A.; Duffy, G. P.; O'Brien, F. J. Combinatorial gene therapy accelerates bone regeneration: non-viral dual delivery of VEGF and BMP2 in a collagen-nanohydroxyapatite scaffold. *Adv. Healthcare Mater.* **2015**, *4*, 223–227.
- (32) Mashal, M.; Attia, N.; Martinez-Navarrete, G.; Soto-Sanchez, C.; Fernandez, E.; Grijalvo, S.; Eritja, R.; Puras, G.; Pedraz, J. L. Gene delivery to the rat retina by non-viral vectors based on chloroquine-containing cationic niosomes. *J. Controlled Release* **2019**, *304*, 181–190.
- (33) Villate-Beitia, I.; Truong, N. F.; Gallego, I.; Zarate, J.; Puras, G.; Pedraz, J. L.; Segura, T. Hyaluronic acid hydrogel scaffolds loaded with cationic niosomes for efficient non-viral gene delivery. *RSC Adv.* **2018**, *8*, 31934–31942.
- (34) Herran, E.; Ruiz-Ortega, J. A.; Aristieta, A.; Igartua, M.; Requejo, C.; Lafuente, J. V.; Ugedo, L.; Pedraz, J. L.; Hernandez, R. M. In vivo administration of VEGF- and GDNF-releasing biodegradable polymeric microspheres in a severe lesion model of Parkinson's disease. *Eur. J. Pharm. Biopharm.* **2013**, *85*, 1183–1190.
- (35) Soto-Sanchez, C.; Martinez-Navarrete, G.; Humphreys, L.; Puras, G.; Zarate, J.; Pedraz, J. L.; Fernandez, E. Enduring high-efficiency in vivo transfection of neurons with non-viral magnetoparticles in the rat visual cortex for optogenetic applications. *Nanomedicine* **2015**, *11*, 835–843.
- (36) Schindelin, J.; Arganda-Carreras, I.; Frise, E.; Kaynig, V.; Longair, M.; Pietzsch, T.; Preibisch, S.; Rueden, C.; Saalfeld, S.; Schmid, B.; Tinevez, J. Y.; White, D. J.; Hartenstein, V.; Eliceiri, K.; Tomancak, P.; Cardona, A. Fiji: an open-source platform for biological-image analysis. *Nat. Methods* **2012**, *9*, 676–682.
- (37) Herran, E.; Requejo, C.; Ruiz-Ortega, J. A.; Aristieta, A.; Igartua, M.; Bengoetxea, H.; Ugedo, L.; Pedraz, J. L.; Lafuente, J. V.; Hernandez, R. M. Increased antiparkinson efficacy of the combined administration of VEGF- and GDNF-loaded nanospheres in a partial lesion model of Parkinson's disease. *Int. J. Nanomed.* **2014**, *9*, 2677–2687.
- (38) Spuch, C.; Antequera, D.; Portero, A.; Orive, G.; Hernandez, R. M.; Molina, J. A.; Bermejo-Pareja, F.; Pedraz, J. L.; Carro, E. The effect of encapsulated VEGF-secreting cells on brain amyloid load and behavioral impairment in a mouse model of Alzheimer's disease. *Biomaterials* **2010**, *31*, 5608–5618.
- (39) Darrow, J. J. Luxturna: FDA documents reveal the value of a costly gene therapy. *Drug Discovery Today* **2019**, *24*, 949–954.
- (40) Martino, M. M.; Brkic, S.; Bovo, E.; Burger, M.; Schaefer, D. J.; Wolff, T.; Gurke, L.; Briquez, P. S.; Larsson, H. M.; Gianni-Barrera, R.; Hubbell, J. A.; Banfi, A. Extracellular matrix and growth factor engineering for controlled angiogenesis in regenerative medicine. *Front. Bioeng. Biotechnol.* **2015**, *3*, 45.
- (41) Gratton, S. E.; Ropp, P. A.; Pohlhaus, P. D.; Luft, J. C.; Madden, V. J.; Napier, M. E.; DeSimone, J. M. The effect of particle design on cellular internalization pathways. *Proc. Natl. Acad. Sci. U. S. A.* **2008**, *105*, 11613–11618.
- (42) Meshnick, S. R. Chloroquine as intercalator: a hypothesis revived. *Parasitol. Today* **1990**, *6*, 77–79.
- (43) Allison, J. L.; O'Brien, R. L.; Hahn, F. E. DNA: reaction with chloroquine. *Science* **1965**, *149*, 1111–1113.
- (44) Cheng, J.; Zeidan, R.; Mishra, S.; Liu, A.; Pun, S. H.; Kulkarni, R. P.; Jensen, G. S.; Belloq, N. C.; Davis, M. E. Structure-function correlation of chloroquine and analogues as transgene expression enhancers in nonviral gene delivery. *J. Med. Chem.* **2006**, *49*, 6522–6531.
- (45) Yang, C.; Hu, T.; Cao, H.; Zhang, L.; Zhou, P.; He, G.; Song, X.; Tong, A.; Guo, G.; Yang, F.; Zhang, X.; Qian, Z.; Qi, X.; Zhou, L.; Zheng, Y. Facile Construction of Chloroquine Containing PLGA-Based pDNA Delivery System for Efficient Tumor and Pancreatitis Targeting in Vitro and in Vivo. *Mol. Pharmaceutics* **2015**, *12*, 2167–2179.
- (46) Yang, Z.; Jiang, Z.; Cao, Z.; Zhang, C.; Gao, D.; Luo, X.; Zhang, X.; Luo, H.; Jiang, Q.; Liu, J. Multifunctional non-viral gene vectors with enhanced stability, improved cellular and nuclear uptake capability, and increased transfection efficiency. *Nanoscale* **2014**, *6*, 10193–10206.
- (47) de Lima, M. C. P.; Neves, S.; Filipe, A.; Duzgunes, N.; Simoes, S. Cationic liposomes for gene delivery: from biophysics to biological applications. *Curr. Med. Chem.* **2003**, *10*, 1221–1231.
- (48) Aly, A. E.; Harmon, B.; Padegimas, L.; Sesenoglu-Laird, O.; Cooper, M. J.; Yurek, D. M.; Waszczak, B. L. Intranasal delivery of hGDNF plasmid DNA nanoparticles results in long-term and widespread transfection of perivascular cells in rat brain. *Nanomedicine* **2019**, *16*, 20–33.
- (49) Aly, A. E.; Harmon, B. T.; Padegimas, L.; Sesenoglu-Laird, O.; Cooper, M. J.; Waszczak, B. L. Intranasal Delivery of pGDNF DNA Nanoparticles Provides Neuroprotection in the Rat 6-Hydroxydopamine Model of Parkinson's Disease. *Mol. Neurobiol.* **2019**, *56*, 688–701.
- (50) Liesz, A. The vascular side of Alzheimer's disease. *Science* **2019**, *365*, 223–224.

(51) Broce, I. J.; Tan, C. H.; Fan, C. C.; Jansen, I.; Savage, J. E.; Witoelar, A.; Wen, N.; Hess, C. P.; Dillon, W. P.; Glastonbury, C. M.; Glymour, M.; Yokoyama, J. S.; Elahi, F. M.; Rabinovici, G. D.; Miller, B. L.; Mormino, E. C.; Sperling, R. A.; Bennett, D. A.; McEvoy, L. K.; Brewer, J. B.; Feldman, H. H.; Hyman, B. T.; Pericak-Vance, M.; Haines, J. L.; Farrer, L. A.; Mayeux, R.; Schellenberg, G. D.; Yaffe, K.; Sugrue, L. P.; Dale, A. M.; Posthuma, D.; Andreassen, O. A.; Karch, C. M.; Desikan, R. S. Dissecting the genetic relationship between cardiovascular risk factors and Alzheimer's disease. *Acta Neuropathol.* **2019**, *137*, 209–226.

(52) Power, M. C.; Mormino, E.; Soldan, A.; James, B. D.; Yu, L.; Armstrong, N. M.; Bangen, K. J.; Delano-Wood, L.; Lamar, M.; Lim, Y. Y.; Nudelman, K.; Zahodne, L.; Gross, A. L.; Mungas, D.; Widaman, K. F.; Schneider, J. Combined neuropathological pathways account for age-related risk of dementia. *Ann. Neurol.* **2018**, *84*, 10–22.

(53) Toledo, J. B.; Arnold, S. E.; Raible, K.; Brettschneider, J.; Xie, S. X.; Grossman, M.; Monsell, S. E.; Kukull, W. A.; Trojanowski, J. Q. Contribution of cerebrovascular disease in autopsy confirmed neurodegenerative disease cases in the National Alzheimer's Coordinating Centre. *Brain* **2013**, *136*, 2697–2706.

(54) Iadecola, C. The overlap between neurodegenerative and vascular factors in the pathogenesis of dementia. *Acta Neuropathol.* **2010**, *120*, 287–296.